Materials Science & Engineering C 110 (2020) 110624

Contents lists available at ScienceDirect

Materials Science & Engineering C

journal homepage: www.elsevier.com/locate/msec

Mussel-inspired polydopamine-assisted bromelain immobilization onto electrospun fibrous membrane for potential application as wound dressing

Xinxin Chen[a,1], Xiang Wang[a,1], Siyu Wang[c], Xiuhang Zhang[a], Jiaao Yu[a,*], Ce Wang[b,*]

[a] Department of Burn Surgery, First Hospital of Jilin University, Changchun, Jilin 130021, PR China
[b] Alan G. Macdiarmid Institute, Jilin University, Changchun, Jilin 130012, PR China
[c] Department of Gastrointestinal Surgery, China-Japan Union Hospital, Jilin University, Changchun, Jilin 130033, PR China

ARTICLE INFO

Keywords:
Bromelain
Electrospinning
Polydopamine
Wound dressing

ABSTRACT

There has been a recent increase in research interest regarding the development of wound dressings containing bioactive compounds capable of improving outcomes for complex healing needs. In the present study, we describe the generation of bromelain immobilized eletrospun poly(ε-caprolactone) (PCL) fibers (BrPDA-PCL fibers) using the dopamine-assisted co-deposition strategy. We wanted to combine the structural advantage of electrospun fiber and the activity of bromelain and PDA to develop functional wound dressings. We found that bromelain activity could be better stabilized when via its immobilization on electrospun fibers. The resultant BrPDA-PCL fibers exhibited promising properties including optimal mechanical stability, wettability, and rates of water vapor transmission. In addition, these BrPDA-PCL fibers were biocompatible, allowing for effective cellular adhesion and proliferation. The results of zone of inhibition testing further confirmed that these fibers achieved effective antibacterial activity against *Escherichia coli* and *Staphylococcus aureus*. When used in vivo, as compared with PCL fibers or control animals the BrPDA-PCL fibers enhanced wound healing rates while reducing associated inflammation. As such, these results indicate that these biocompatible BrPDA-PCL fibers exhibit desirable physicochemical properties making them ideal for use as a wound dressing to enhance the repair of full-thickness wounds to the skin.

1. Introduction

Skin damage as a result of injury, be it acute or chronic, can adversely impact the quality of life of affected individuals, with serious wounds being life-threatening in certain cases, leading to a high clinical demand for effective wound dressing materials [1,2]. Effective wound dressings are those which maintain moisture in the wound site, maintaining hemostasis while preventing the development of any infections, thereby allowing air and water to more effectively facilitate epithelization [3,4]. At present the bioactivity of most wound dressings is relatively poor, with more effective dressings being very costly and difficult to produce, necessitating the development of novel wound healing materials. Recent research has highlighted the potential of electrospun fibrous membranes as a material for use in wound dressing design [5]. Membranes designed using electrospinning technology have desirable features including a pore size that is readily tunable, as well as substantial air permeability and a high surface-to-volume ratio. These membranes also have a 3D structure that is similar to the structure of the extracellular matrix (ECM), which is essential for mediating effective cellular adhesion and proliferation. These advantageous properties make such electrospun fibers potentially ideal for use in wound dressings [6]. Studies have further sought to functionalize these fibers so as to enhance their ability to promote wound healing via imbuing them with growth factors, antibacterial compounds, or other bioactive materials [7–10]. Therefore, the exploration and development of new bioactive materials for electrospun fiber functionalization to regulate the wound healing is of great significance.

Given their safety and relatively low cost, bioactive plant extracts have been the subject of particular interest in the context of wound healing. One such extract is bromelain, which is a crude extract isolated from the pineapple fruit that contains a number of therapeutically valuable proteolytic enzymes [11]. Previous work has shown bromelain to be capable of mediating anti-inflammatory and anti-edematous properties in many contexts including sinusitis, thrombophlebitis, angina pectoris, bronchitis, surgical trauma, and pyelonephritis [12]. Bromelain is also known to be capable of hydrolyzing devitalized tissues so as

* Corresponding authors.
E-mail addresses: yujiaao1973@126.com (J. Yu), cwang@jlu.edu.cn (C. Wang).
[1] These two authors contribute equally to this work.

https://doi.org/10.1016/j.msec.2019.110624
Received 9 August 2019; Received in revised form 15 December 2019; Accepted 31 December 2019
Available online 07 January 2020
0928-4931/

to enhance rates of wound healing [13]. Efforts to maintain the stability of bromelain are essential for its therapeutic utilization, with previous groups having demonstrated that bromelain can be effectively incorporated into electrospun or other polymer matrices. For example, Bayat et al. were able to use a blending electrospinning process to generate chitosan nanofibers loaded with bromelain [14], while Korrapati et al. used coaxial electrospinning in order to incorporate bromelain into electrospun fibers [15]. In addition to direct incorporation, bromelain can also be immobilized directly onto the surface of electrospun fibers, allowing for more direct interaction between bromelain and wound tissue. Unfortunately, electrospun fibers tend to interact poorly with enzymes, resulting in relatively poor enzymatic activity and stability. Therefore, there is a need to develop better techniques for immobilizing bromelain onto electrospun fibers.

Previous studies have highlighted the potential of mussel-inspired polydopamine (PDA), which is produced via the oxidative polymerization of dopamine, as a substrate with the potential for utilization in the development of advanced biomaterials [16,17]. Recently, PDA has also shown its potential application in skin regeneration [18]. As a mussel-inspired material, PDA possesses many properties, such as a simple preparation process, good biocompatibility, strong adhesive property and easy functionalization. In addition, PDA has attracted increasingly considerable attention because it provides a simple and versatile approach to functionalize material surfaces without the need of expensive or complex instruments and procedures [19]. Importantly, PDA is highly versatile owing to the abundance of available functional groups, allowing it to be developed into a platform well-suited to use in myriad applications [20]. PDA has been shown to ameliorate enzymatic immobilization via both Schiff base reactions and Michael-type addition [21,22]. However, at present there are no reports regarding the potential for PDA to facilitate bromelain immobilization.

In the present report we describe the successful use of PDA to mediate bromelain immobilization on electrospun fibers through the co-deposition strategy, with the resultant fibers being effective when used for dressing wounds (Scheme 1). We wanted to combine the structural advantage of electrospun fiber and the therapeutic effects of bromelain and PDA to develop functional wound dressings. The synthetic polymer poly(ε-caprolactone) (PCL), which exhibits good biocompatibility, was selected for use as a matrix that was used to generate a fibrous membrane onto which bromelain could be immobilized. The FDA has approved the biomedical use of PCL, and it has previously been shown to exhibit both a high degree of mechanical stability while also remaining biodegradable [23]. In this report, bromelain and PDA could be immobilized onto the fibers via one-step reaction. The physical and chemical properties of obtained electrospun fiber membranes were characterized. Meanwhile, the activity and stability of immobilized bromelain was also investigated systematically. We additionally assessed the utility of these membranes as mediators of cellular adhesion, cell proliferation, and antibacterial activity in vitro, and as drivers of enhanced wound healing in vivo. Together our findings highlight these bromelain-immobilized electrospun PCL fiber membranes as having great promise for use in wound healing applications.

2. Materials and methods

2.1. Materials

PCL (Mw = 80,000), pineapple stem-derived bromelain, Calcein-AM, and the Alamar Blue Assay were obtained from Sigma-Aldrich. Dichloromethane and acetone aniline were purchased from Tiantai Chemical Corp. Tris(hydroxymethyl)aminomethane hydrochloride (Tris) was from Energy Chemical. Dopamine hydrochloride (DA) was from Aladdin. *S. aureus* (ATCC 25923), *E. coli* (ATCC 25922) bacteria as well as the bouillon culture-medium were obtained from the First Hospital Microbiology laboratory of Jilin University. Unless otherwise stated, all chemicals were analytical grade, and deionized water was used for all experiments.

2.2. Electrospun PCL fiber production

PCL granules were dissolved in a 4:1 (mass ratio) dichloromethane and acetone solution to yield the PCL (8 wt%) solution. This solution was then placed within a glass syringe attached to a high-voltage power supply, and a 15-kV potential was provided between the cathode and anode at a distance of 20 cm to prepare PCL fibers.

2.3. Bromelain-immobilized PCL fiber generation

Ethanol was first used to wet 50 mg of PCL fibers (owing to their hydrophobicity), and fibers were then soaked in a 50 mL volume of a solution containing dopamine (2.0 mg/mL) and bromelain (1.0 mg/mL) with continuous stirring for 8 h at 25 °C. The dopamine and bromelain concentrations were determined through a preliminary study. When dopamine was polymerized to polydopamine, bromelain was *in-site* bonded to the PDA layer and then onto immobilized the fibers. After the reaction, fibers were washed in distilled water to release weakly-

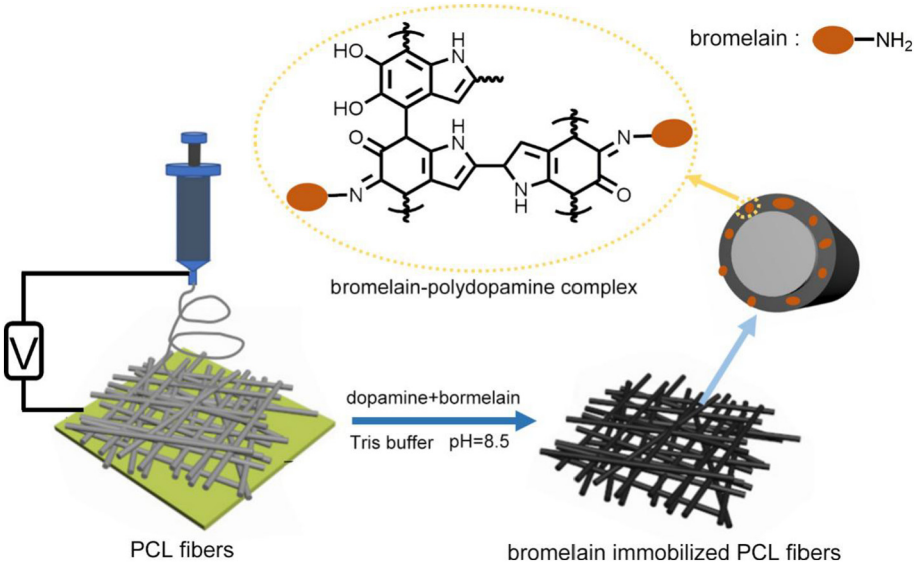

Scheme 1. Overview of the procedure used to synthesize bromelain-immobilized electrospun PCL fibers with the help of PDA.

attached bromelain. The prepared fibers were placed in the desiccator before use. In parallel, PDA-coated PCL fibers were also prepared without addition of bromelain.

2.4. Fiber characterization

Field-emission scanning electron microscopy (SEM, FEI Nova NanoSEM) was used to analyze the morphology of fibers. Mean fiber diameter and distribution was assessed based on measurements of 100 fibers using the Image-ProPlus software package. For transmission electron microscopy (TEM; Hitachi S-570), a 100 kV accelerating voltage was used. A Bruker Vector-22 spectrometer was used at room temperature to assess FT-IR spectra from 4000 to 400 cm^{-1} with powder-pressed KBr pellets at room temperature, while a Thermo ESCALAB 250 spectrometer was used to assess X-ray photoelectron spectra (XPS) with a Mg—K (1253.6 eV) achromatic X-ray source. To assess mechanical properties, 40 mm × 10–15 mm fiber membranes were held between a pair of stainless steel clamps (tensile speed = 20 $mm{\cdot}min^{-1}$) with a mechanical strength tester (YG026H, Wuhan National Instrument Co., Ltd., China). A contact angle analyzer (Surface Electro Optics Co., Korea) was used to determine water contact angle.

2.5. Swelling test

In order to measure the ability of fibers to absorb solutions in a manner similar to that which would occur in wound sites, 20 mg fiber pieces were cut into three equal sections and soaked at 37 °C in a 20 mL volume of PBS. At the indicated time point, fibers were removed from solution and filter paper was used to remove excess water prior to sample weight. The degree of swelling was calculated as follows:

$$\text{Degree of swelling\%} = \frac{W_w - W_d}{W_d} \times 100 \quad (1)$$

with W_w and W_d as the weight (mg) of wet and dry fibers, respectively.

2.6. Water vapor transmission rates (WVTR) and biodegradation test

The ASTM E96 (American Society for Testing Materials)-standard approach was used to WVTR measurements [7]. Briefly, a cylindrical beaker containing 15 mL deionized water was sealed using the membranes of interest and then incubated in a test chamber set to 37 °C with 40 ± 2% relative humidity. The beaker was measured once hourly for 24 h, with weight loss being recorded and the corresponding slope determined as follows:

$$\text{WVTR} = \frac{\text{slope}\times 24}{A} g/m^2/\text{day} \quad (2)$$

with A as sample test area (m^2). Samples were assessed for WVTR values a minimum of 4 times.

The biodegradability of obtained fibers was tested in vitro in PBS (pH = 7.4) for 5 weeks at 37 °C. Fiber samples were taken out from the solution every week, washed with distilled water and dried. The weight change before and after drying was used to evaluate the degradation rate.

2.7. In vitro bromelain release and loading

In order to assess rates of bromelain release from bromelain-immobilized fibers, a 1.5 × 1.5 cm mass of fibers (5 mg) was added to 20 mL PBS (pH 7.4) at 37 °C. At defined time points, 1.0 mL was removed from this solution and was replaced with an equivalent volume of PBS. The BCA assay was used to measure bromelain levels in collected test samples, with bromelain loading efficiency determined based on cumulative bromelain release.

2.8. Enzyme activity and stability

The enzymatic activity of bromelain was assayed as described previously [15]. Briefly, samples containing bromelain were incubated in a 1 mL solution containing 0.2 M phosphate buffer (pH 7.4, 0.25 mL), 5 mM cysteine-HCL (0.25 mL), and 1% (w/v) casein (0.5 mL) for 30 min, after which 1 mL 15% TCA was added to terminate reactions, after which samples were centrifuged. Precipitates were collected, filtered through Whatman No. 1 filter paper, and absorbance at 280 nm was measured. Units of activity per mg protein were used to measure enzymatic specific activity. Free and immobilized bromelain stability was assessed via storing fibers or free bromelain at 4 °C for indicated time points, after which samples were isolated and incubated in 1 mL PBS for 4 h at 37 °C with shaking. Enzymatic activity was then assessed as above.

2.9. In vitro cytotoxicity and cell observation

The Alamar Blue Assay was used to assess the effects of fiber samples on L929 fibroblast viability. First, fiber membranes (1 cm diameter) underwent UV irradiation to sterilize them for ~1 h per side, after which they were added to fresh cell culture media (DMEM containing 10% PBS and 1% streptomycin/penicillin) in a 24-well plate for 24 h at 37 °C in a 5% CO_2 incubator. L929 cells were added to wells of these 24-well plates in a 1 mL volume of cell culture media (10,000 cells/well) and were allowed to incubate for an additional 4, 24, or 48 h. A 1:10 solution of Alamar blue was then prepared by diluting the 0.1 mg/mL stock solution using serum-free DMEM. A total of 200 μL of this solution was then added per well of a 96-well plate, and absorbance at 570 nm and 600 nm was then measured in triplicate. A provided formula was used to calculate the percentage of Alamar Blue reduction, with viability determined as a percentage of untreated control samples. In fluorescence microscopy experiments, after a 72 h incubation a 20 μL solution of Calcein-AM (30 μM, Sigma) was added per well into 200 μL DMEM, and samples were allowed to incubate in the dark for 30 min in a 37 °C incubator. Fibers were then washes carefully twice with PBS, and fluorescence microscopy was used to assess cell attachment (excitation: 445–495 nm) on a Nikon Eclipse LV100. For SEM measurements, 2.5% glutaraldehyde was used to fix cells, which were then washed thrice using PBS and dehydrated with an ethanol gradient (30, 50, 70, 85, 90, and 100% respectively, 20 min per concentration). Cells were then freeze dried prior to SEM assessment.

2.10. Assessment of antibacterial activity

The Kirby–Bauer (K—B) disc method was used for gauging membrane antibacterial activity. Briefly, 8 mm diameter discs were created for each fiber sample. Agar plates containing bouillon culture-media were then inoculated with a 1 mL bacterial suspension of 10^5 colony forming units (CFUs) of either *Escherichia coli* (Gram-negative) or *Staphylococcus aureus* (Gram-positive). Fiber discs were then carefully placed onto these plates, which were allowed to incubate for 24 h at 37 °C, after which the zone of clearing around each fiber sample was measured. Image-pro Plus was used to determine the average zone of inhibition.

2.11. In vivo wound healing model

To assess the ability of fiber wound dressing to facilitate wound healing, a full-thickness excision wound model was established. All animal studies received approval from the ethical committee of Jilin University, and were performed in a manner consistent with the direct suggestion of care for laboratory animals approved by the Ministry of Science and Technology of China. For this model, 2-month-old male Sprague Dawley (SD) rats (200–250 g) from the Laboratory Animal Centre of Jilin University were used. Animals were individually housed

under standard conditions, with a 12 hour dark/light cycle and free food/water access. Animals were anesthetized using chloral hydrate (10%, 0.3 mL/100 g body weight), which was injected intraperitoneally. Dorsal hair was then shaved, and a scalpel was used to generate the wound that extended into the loose subcutaneous tissue. Animals that underwent wounding were then separated at random into 3 groups (n = 3/group) and were treated via application of either PCL fiber, bromelain-immobilized PCL fiber, or no dressing. Dressings were sutured to the wound area, and healing was monitored throughout the wound recovery process.

2.12. Histology and immunohistochemistry (IHC)

For histology, wound site samples were collected 7 days after wounding and were fixed using 10% formalin, after which they were paraffin-embedded and stained using hematoxylin and eosin (H&E) or IHC approaches. For H&E staining, tissue samples were added to 10% formaldehyde, washed in distilled water, and then stained with hematoxylin after which they were again washed, treated with 0.3% acid alcohol for differentiation, and then rinsed and stained for 2 min with eosin. Samples then underwent dehydration, clearing, and mounting prior to assessment via light microscopy (Nikon Eclipse E400, Japan). For IHC, samples were embedded into optimal cutting medium and frozen using liquid nitrogen, after which 5 μm sections were fixed using 4% paraformaldehyde, blocked using 5% horse serum, and stained for 2 h using antibodies against TNF-α (1:200) or IL6 (1:100). Sections were then washed and stained for 45 min with an appropriate biotinylated secondary antibody with the Vectastain ABC Kit protocol (Vector Laboratories, CA, USA). Samples were then washed again in PBS, and DAB was used to visualize antibody staining, with hematoxylin for counterstaining. Quantification of the positively stained regions for TNF-α and IL6 was performed using the image analysis software Adobe Photoshop CS6 (Adobe, Dublin, Ireland). The colour gamut of positive staining was determined with the colour picker tool and a tolerance of 40. The positively stained pixels were counted in the histogram and calculated against all pixels of the image to determine the percentage of positively stained area [24].

2.13. Statistical analysis

Data are means ± standard deviations. Data normality was assessed via the Shapiro-Wilk test, after which Student's *t*-tests were used to compare results, with $p < 0.05$ as the threshold of significance.

3. Results and discussion

3.1. Fiber morphology

We began by using SEM to compare the morphology of different electrospun fibers, including PCL fibers alone, PDA-coated (PDA-PCL) fibers, and bromelain-immobilized electrospun PCL (BrPDA-PCL) fibers. This analysis revealed all fibers to be long and continuous (Fig. 1), with PCL fibers being smooth and 414 ± 46 nm in diameter on average. The fiber surfaces were visibly coarser following PDA or bromelain immobilization, with increased adherence between fibers as a result of the PDA deposition, with average fiber diameters increasing to 472 ± 41 nm and 517 ± 35 nm, respectively. The surface of BrPDA-PCL fibers was visibly coarser than that of PDA-PCL fibers, with more particulate aggregates likely attributable to the bromelain co-deposition. We further used TEM to assess fiber morphology (Fig. 2). This analysis revealed that both PDA-PCl and BrPDA-PCL fibers exhibited a coarse surface consistent with successful deposition of PDA with or without bromelain onto the surface of these electrospun fibers, consistent with SEM results.

3.2. Characterization of chemical and physical properties

We next used FT-IR spectral results to verify successful PDA and bromelain functionalization of these fibers (Fig. 3a). The results demonstrated that all fibers exhibited the characteristic PCL carboxyl group peak at 1720 cm^{-1} [25]. For pure PCL fibers, the spectrum also showed other characteristic peaks of PCL, such as at 2939 cm^{-1} (asymmetric CH_2 stretching), 2865 cm^{-1} (symmetric CH_2 stretching), 1294 cm^{-1} (C—O and C—C stretching), 1238 cm^{-1} (asymmetric C–O–C stretching), 1159 cm^{-1} (symmetric C–O–C stretching) and 731 cm^{-1} (CH_2 stretching). PDA-PCL fibers exhibited the characteristic bands of PCL and other peaks for PDA. The peaks at 1580 cm^{-1} and 1470 cm^{-1} were attributed to benzene skeleton vibrations. The peak at around 1293 cm^{-1} belonged to primary amine and C—O stretching vibration [26]. The spectrum of bromelain was also obtained and is shown in Fig. S1. Pure bromelain showed peaks at 1225 cm^{-1} and 1515 cm^{-1} belonging to C═N groups from the non-conjugated amines. The peak at 1652 cm^{-1} was assigned to the C═O band from the amide I. The peak at 3320 cm^{-1} belonged to the N—H stretching of a secondary N-substituted amide [14]. BrPDA-PCL fibers exhibited the characteristic peaks of PCL and PDA. Most of the characteristic peaks for bromelain overlapped with those for PCL and PDA. However, it can be observed that the peak at 3320 cm^{-1} in bromelain shifted to 3310 cm^{-1} in BrPDA-PCL fibers and the peak at 1652 cm^{-1} in bromelain also moved to 1640 cm^{-1}. These results suggest that bromelain has been immobilized onto the fibers through the bonding between PDA and bromelain. Fiber chemical composition was further gauged via XPS (Fig. 3b). PCL fibers display C 1s and O 1s peaks at 284.5 eV and 532.8 eV, without any evidence of N content. In contrast both the PDA-PCL and BrPDA-PCL fibers exhibited a clear N 1s binding energy peak at ~400.1 eV, given that both PDA and bromelain contain nitrogen. In addition, BrPDA-PCL fibers exhibited S 2s and S 2p peaks at 235.4 eV and 166.3 eV owing to the cysteine content of bromelain [27]. Changes in fiber chemical structures were further confirmed based upon elemental percentages derived from XPS analyses (Fig. 3c). Together these results confirm that we were able to successfully immobilize bromelain on the surface of PCL fibers using PDA.

A number of key mechanical properties are essential determinants of the efficacy of wound dressing materials, leading us to study properties including mechanical strength, wettability, water vapor transmission rate, and swelling behavior in Fig. 4. The PCL fibers exhibited a tensile strength of 5.2 ± 0.9 MPa with an 85.1 ± 3.2% elongation break, whereas PDA and Br-PDA coating increased tensile strength to 6.1 ± 1.1 MPa and 6.0 ± 1.3 MPa, respectively, owing to inter-fiber adhesion, and decreased the elongation breaks to 34.8 ± 4.1% and 45.3 ± 3.7%, respectively (Fig. 4a). The wound is a moist environment; thus, it is necessary to evaluate the mechanical properties of the fibers in wet conditions. The wet fibers were obtained after the fibers were soaked in PBS for 1 week. As shown in Fig. S2, the tensile strength had a decreasing trend and the elongation at break had an increasing trend for the wet samples. The adsorbed water on the wet fibers would make the materials more flexible [28]. Thus, the elongation at break increased and the tensile strength decreased accordingly. However, the mechanical properties for dry and wet samples could meet the requirements of actual usage. These results suggest that the BrPDA-PCL fibers are able to retain good integrity, thus enabling them to maintain patient comfort while minimizing the risk of secondary damage to the wound site. Given that tissue engineering scaffold hydrophilicity has a strong impact on local cell attachment, the wettability of wound dressings is a key design consideration [29]. PCL fibers had a 132° water contact angle (Fig. 4b), consistent with a high degree of hydrophobicity, whereas the hydrophilic nature of PDA and bromelain reduced these angles to 21° and 20° for PDA-PCL and BrPDA-PCL fibers, respectively. As such these wound dressings are suitably hydrophilic, allowing for better cell adhesion and spreading at the wound site. Tissue scaffold swelling is also a key consideration in wound dressing

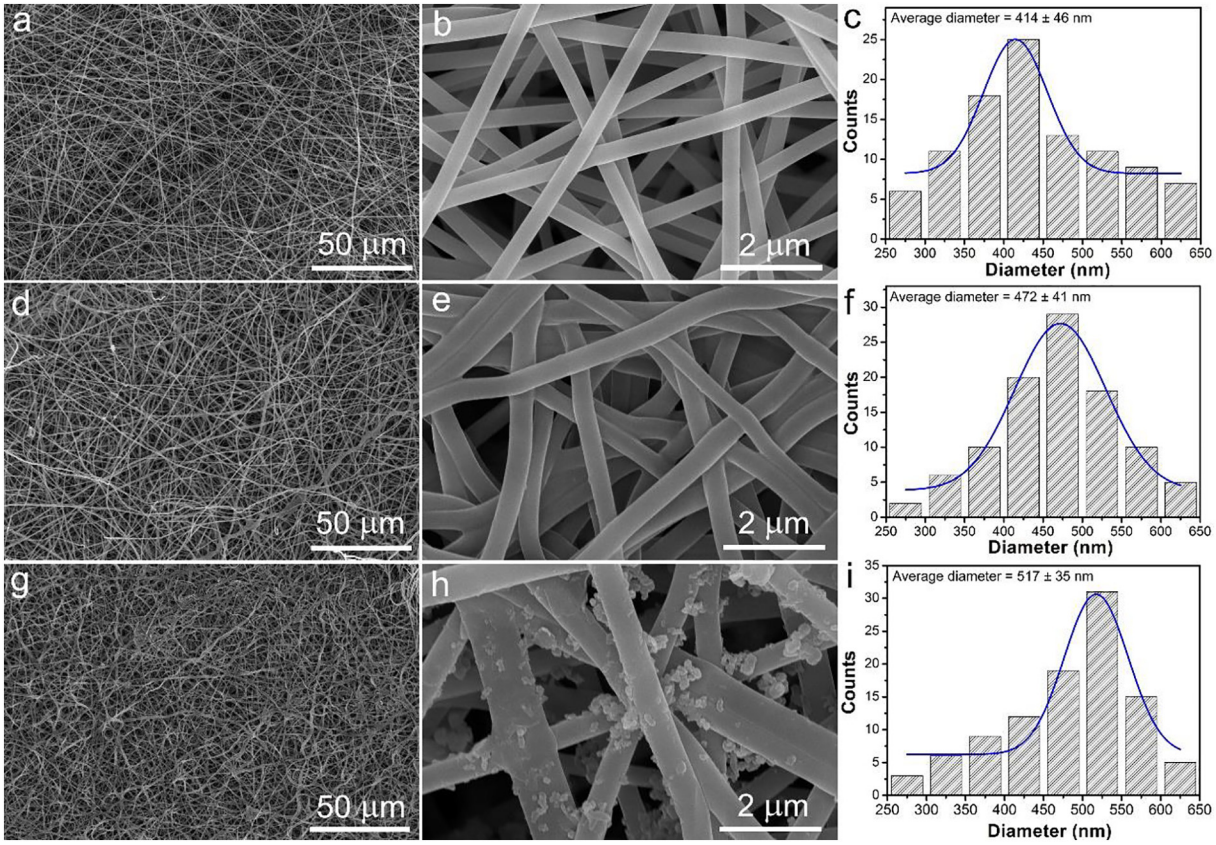

Fig. 1. SEM images and diameter distributions of (a–c) PCL fibers, (d–f) PDA-PCL fibers and (g–i) BrPDA-PCL fibers.

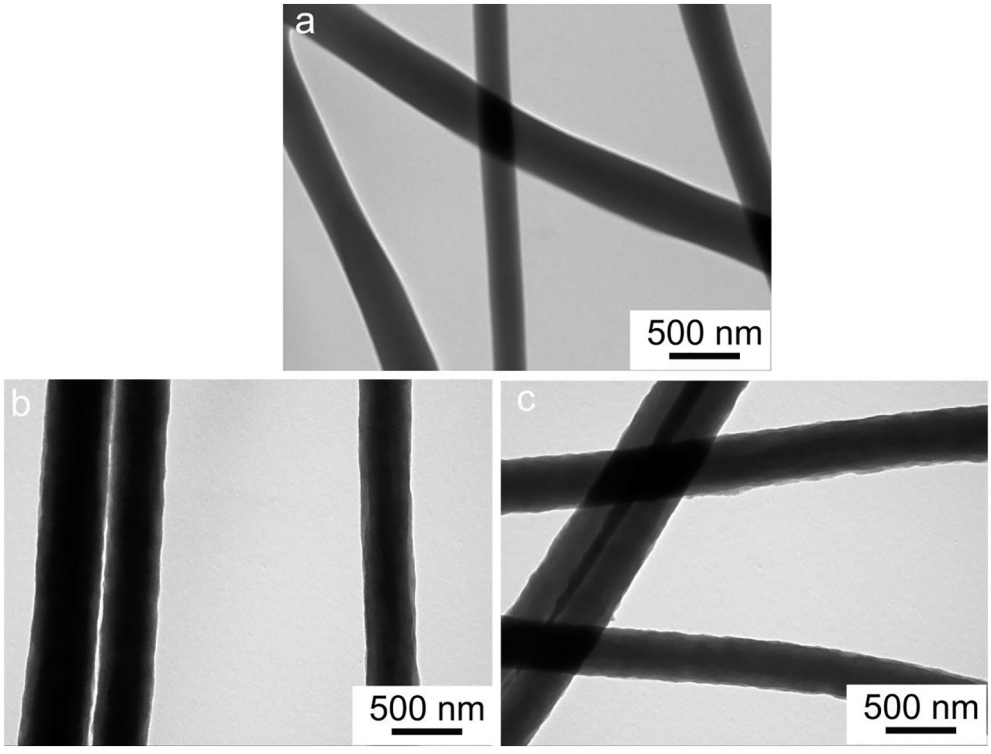

Fig. 2. TEM images of (a) PCL fibers, (b) PDA-PCL fibers, and (c) BrPDA-PCL fibers (the scale bars in the figures are all 500 nm).

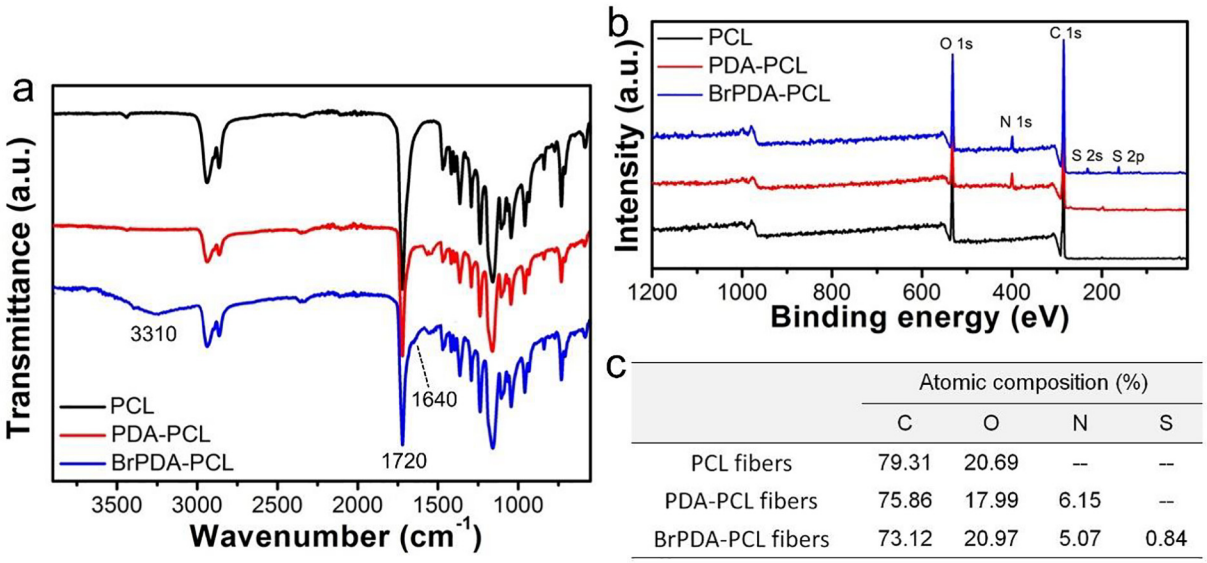

c

	Atomic composition (%)			
	C	O	N	S
PCL fibers	79.31	20.69	--	--
PDA-PCL fibers	75.86	17.99	6.15	--
BrPDA-PCL fibers	73.12	20.97	5.07	0.84

Fig. 3. (a) FTIR spectra, (b) XPS spectra and (c) surface chemical composition of PCL, PDA-PCL, and BrPDA-PCL fibers.

design, given that swelling can allow these scaffolds to absorb local exudates at the wound site. We therefore tested the water absorption of these different fiber materials (Fig. 4c). We found that over a 24 h period, PCL fibers exhibited 40.9% swelling, whereas the swelling of the PDA-PCL and BrPDA-PCL fibers increased to 84.1% and 86.1%, respectively, as a consequence of their desirable hydrophilicity. The higher swelling of BrPDA-PCL fibers may be attributed to their better hydrophilicity. It is also vital that rates of water evaporation from wound sites be carefully controlled to optimize healing, with previous studies suggesting that the WVTR of an effective wound dressing should be in the 76–9360 g/m^2/day range, depending on the specific materials utilized [30]. The skin normally has a water vapor loss rate of 204 ± 12 g/m^2/day, while for first degree burns this increases to 279 ± 26 g/m^2/day, and for granulation wounds it rises to

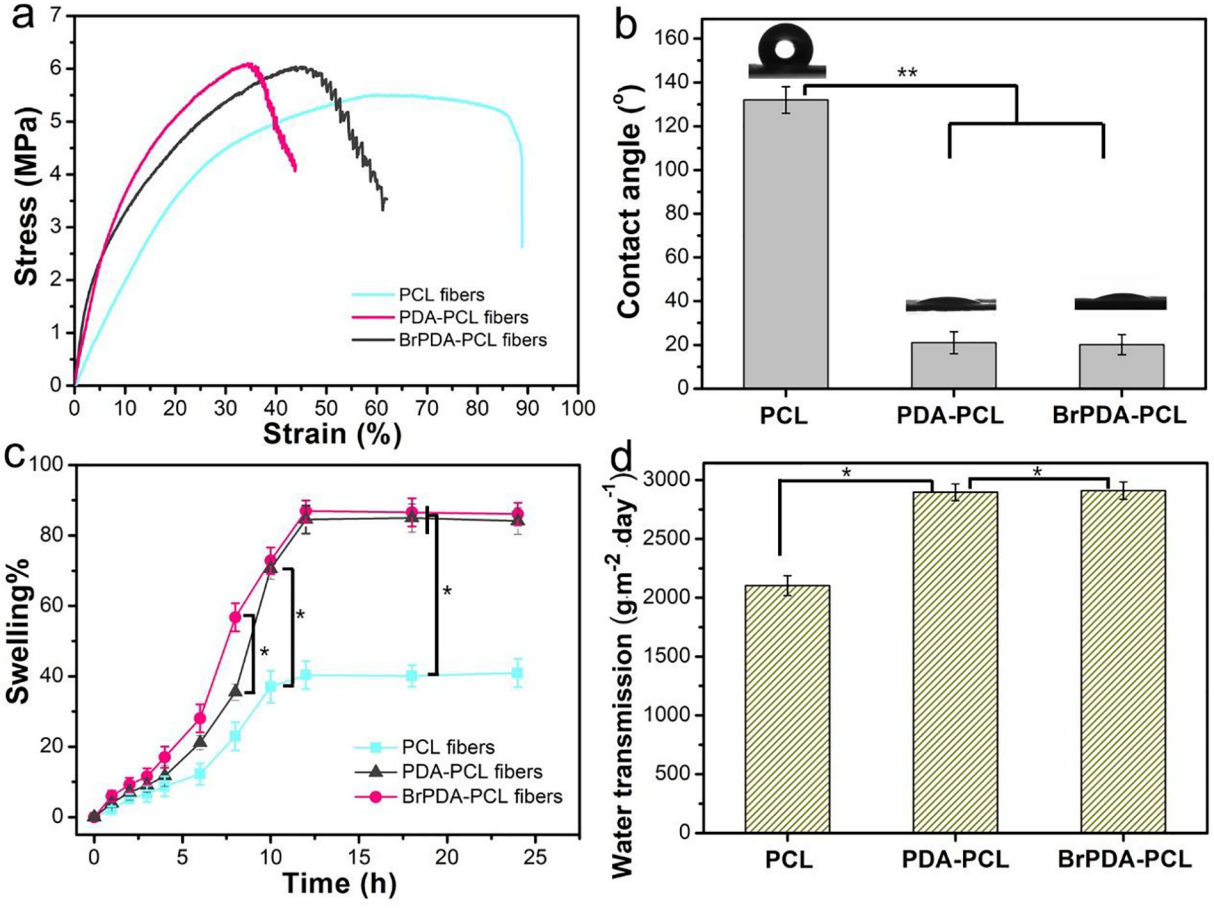

Fig. 4. Mechanical properties (a), water contact angles (b), swelling properties (c) and water vapor transmission rates (d) of the fibers. *p < 0.05, **p < 0.01.

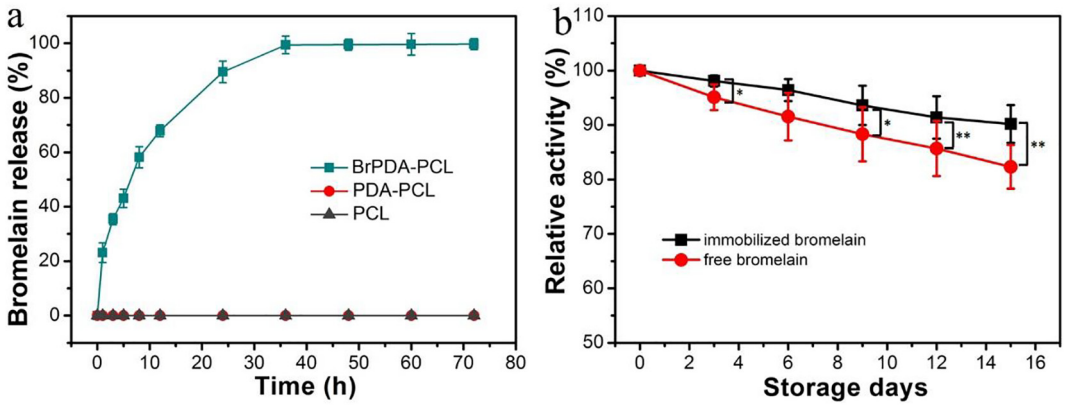

Fig. 5. (a) Release of bromelain from BrPDA-PCL fibers, and (b) long-term stability of bromelain immobilized onto PCL fibers, relative to free bromelain. *p < 0.05, **p < 0.01.

5138 ± 202 g/m^2/day. Generally, in order to maintain adequate moisture at the wound site a rate of 2000–2500 g/m^2/day is recommended to improve wound healing, with higher WVTR rates leading to more rapid wound drying and scar formation and lower rates leading to exudate accumulation, potentially allowing for bacterial growth and delayed healing. We found that BrPDA-PCL fibers exhibited a ~2900 g/m^2/day WVTR, which is close to the recommended range for ideal wound dressings (Fig. 4d). The fiber weight loss in PBS solution was tested to evaluate their degradation rate. As displayed in Fig. S3, PCL fibers and PDA-PCL fibers showed almost no degradation because of the slow degradation rate of PCL and PDA, which is in agreement with the literature report [31,32]. BrPDA-PCL fibers showed 12% degradation which is mainly attributed to the released bromelain. The results indicated that the good integrality of the fibers could ensure the security during the usage. Together these findings thus show that BrPDA-PCL fibers exhibit desirable properties that may make them ideal for wound dressing applications.

3.3. In vitro assessment of bromelain release and stability

The rate of bromelain loss from these composite fiber materials can offer insight into optimal timing of wound dressing changes. As expected, bromelain release from PCL and PDA-PCL fibers was not detectable, whereas BrPDA-PCL fibers continuously released bromelain in two stages: a rapid release (67.5%) over the first 10 h, followed by a slower and more stable release (Fig. 5a). After 3 days, nearly 100% of bromelain was lost from these fibers. Based on calculations, we were able to determine that approximately 100 mg of bromelain was loaded per gram of fibers. It means that the mass fraction of bromelain in the composite fibers is 10 wt%. We additionally assessed the stability of bromelain activity in BrPDA-PCL fibers relative to free bromelain, revealing that while free bromelain activity decreased significantly over a 10 day period, immobilized bromelain activity was largely unchanged for over 15 days (Fig. 5b). Together these results suggest that the deposition of bromelain on electrospun fibers can effectively improve its long-term enzymatic activity.

3.4. Assessment of in vitro cytotoxicity, cell adhesion, and antibacterial efficacy

Tissue scaffolding materials must be biocompatible, and as such we assessed the effects of our fibers on the viability of L929 fibroblasts via the Alamar blue assay, which assessed mitochondrial activity and cellular viability in order to gauge the cytotoxicity of particular compounds. Alamar blue itself is a cell-permeable and non-toxic compound that undergoes mitochondrial reduction, producing a red and highly fluorescent compound (resorufin) [33]. Over the course of cell viability

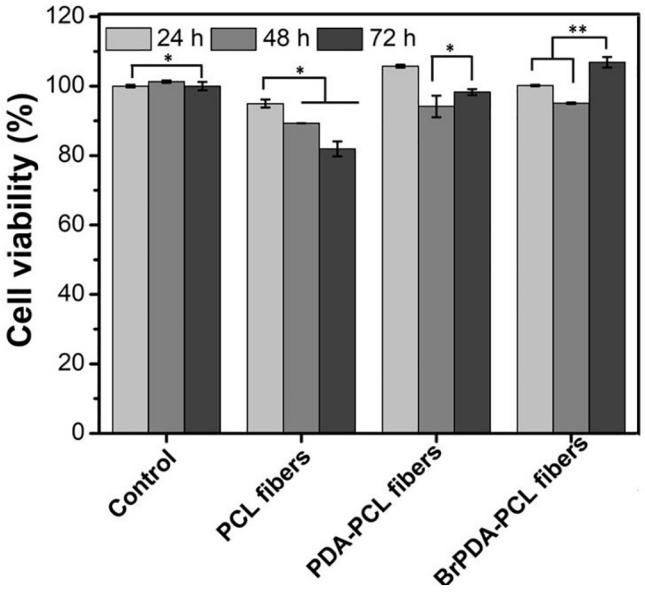

Fig. 6. L929 cell viability as measured via Alamar Blue Assay after incubation with different fiber samples. *p < 0.05, **p < 0.01.

assays, cell densities increased in all sample culture conditions (Fig. 6). We observed no apparent decrease in cell viability when cells were exposed to BrPDA-PCL fibers relative to controls, indicating that these fibers are biocompatible. Indeed, they exhibited superior biocompatibility relative to PCL fibers owing to the hydrophilic nature of the PDA coating which offers a surface for superior cellular adhesion. We additionally used SEM and fluorescence microscopy to assess cellular morphology after a 3 day growth period (Fig. 7). Upon examination, cells appeared healthy with normal spindle-like bipolar morphology and extension. These results thus indicate that BrPDA-PCL fibers offer an ideal biocompatible platform that promotes cellular attachment and proliferation, thus making them potentially ideal for the design of wound dressings.

It is also important that wound dressings achieve antibacterial activity, and as such we used a disc diffusion method to assess the ability of test fibers to prevent the growth of model Gram-negative and Gram-positive bacteria (*E. coli* and *S. aureus*, respectively). In the initial stage of chronic wound formation, Gram-positive bacteria, especially *S. aureus*, are dominant. In addition, staphylococcus and streptococcus are also found in 50% of chronic wounds. Therefore, the prevention and treatment of Staphylococcus is an important factor to initiate wound healing mechanism in wound healing, especially in infected wound [34]. We observed no significant antibacterial activity for the PCL

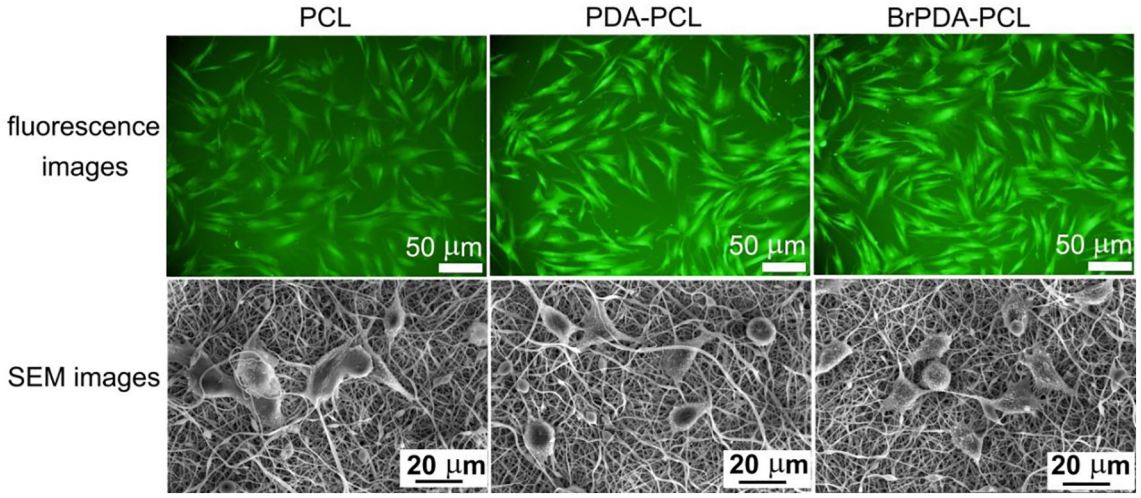

Fig. 7. Fluorescence and SEM images of L929 cells on different fiber samples.

fibers, whereas the PDA-PCL fibers exhibited a pronounced inhibition zone associated with the prevention of the growth of both types of bacteria (Fig. 8), attributable to reactive oxygen species generation by PDA [35]. Consistent with the antimicrobial activity exhibited by bromelain [36], BrPDA-PCL fibers exhibited an even larger zone of inhibition for both bacteria. As such, the synergy between PDA and bromelain make BrPDA-PCL fibers highly effective as an antibacterial wound dressing capable of preventing wound infections.

3.5. *In vivo* wound healing performance

Based on these promising results, we next used a rat model of full-thickness wound healing to assess the relative benefits of BrPDA-PCL fibers in a wound healing application, recording wound healing at 0, 3,

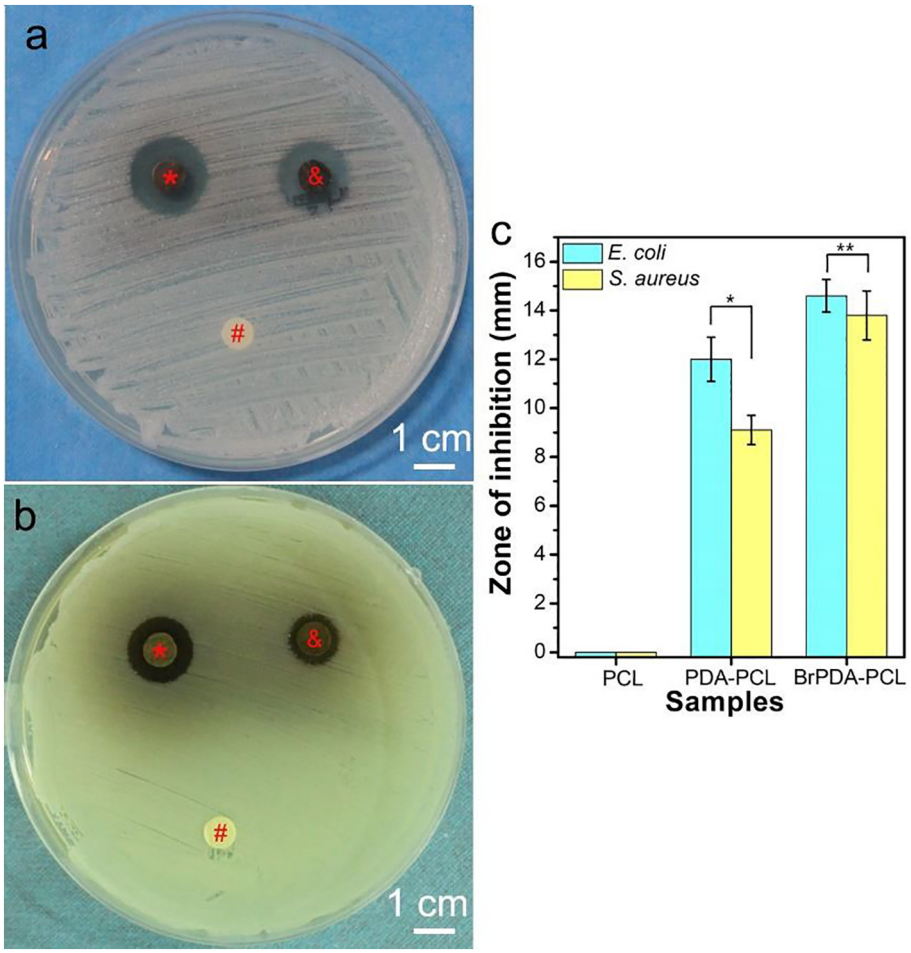

Fig. 8. Antibacterial activities of (#) PCL fibers, (&) PDA-PCL fibers and (*) BrPAD-PCL fibers against *E. coli* (a) and *S. aureus* (b). (c) Inhibition zone results. *p < 0.05, **p < 0.01.

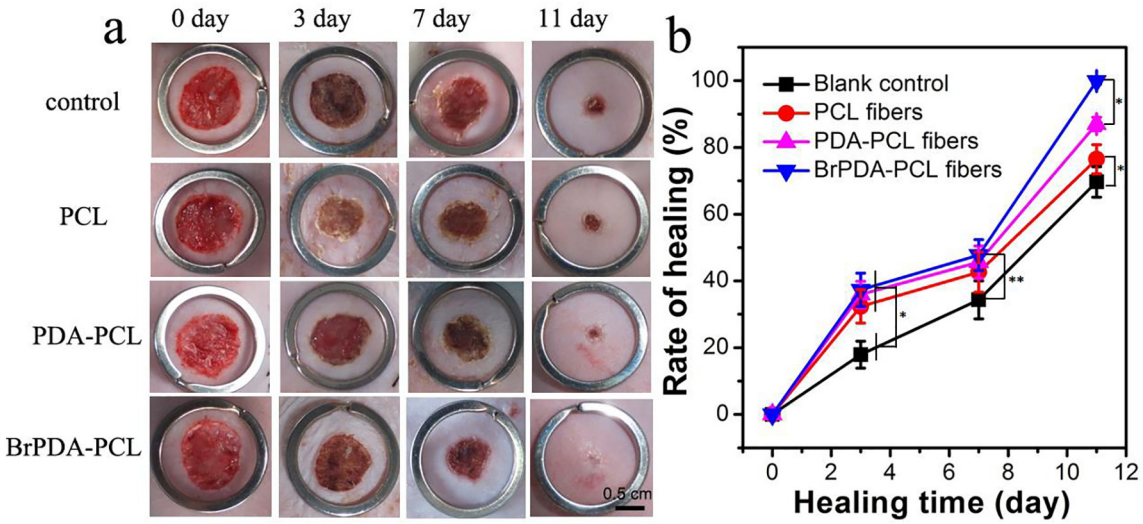

Fig. 9. (a) Representative images of wounds in different treatment groups at different observation time points and (b) wound size reduction in each group. *p < 0.05, **p < 0.01.

7, and 11 days post-wounding (Fig. 9). Relative to control animals, those treated with PCL fibers exhibited superior wound healing, indicating that PCL fibers along are sufficient to mediate enhanced wound closure owing to the fibrous morphology of electrospun fibers, which is more similar to that of the extracellular matrix. In addition, the wounds treated with PDA-PCL fibers showed better healing processes than those treated with PCL fibers. The results are consistent with the previous report that PDA coating could enhance the wound healing effect [18]. Importantly, healing rates were fastest among animals treated using BrPDA-PCL fibers, indicating that PCL functionalization using PDA and bromelain can accelerate the wound healing process. Wounds treated using BrPDA-PCL fibers also appeared substantially flatter following the healing process.

3.6. Histological analyses

We next conducted a histological assessment of wound tissues following the healing process, with H&E staining results shown in Fig. 10a. The magnified images are shown in Fig. S4. There was no obvious evidence of inflammation in response to fibers, with no clear changes relative to control samples. There was an apparent continuous fibrous structure that adhered smoothly to the edge of the material, with limited mononuclear cells and red blood cells present within the tissue, and limited infiltration of these cells into the subcutaneous tissue, possibly as a result of mechanical damage. Both granulocytes and macrophages were evident within fiber dressings during this stage of inflammatory response.

We additionally conducted IHC staining for TNF-α and IL-6 in tissues (Fig. 10b,c). These inflammatory cytokines influence the expression of matrix metalloproteinases (MMPs), thereby regulating tissue healing, in addition to regulating many other aspects of inflammatory responses. We observed a significant improvement in apparent wound perfusion in tissues treated with BrPDA-PCL fibers, without any increase in expression of TNF-α or IL-6 relative to control tissues. All samples were similar in appearance to those of the control group. Compared with PCL group and PDA-PCL group, BrPDA-PCL group

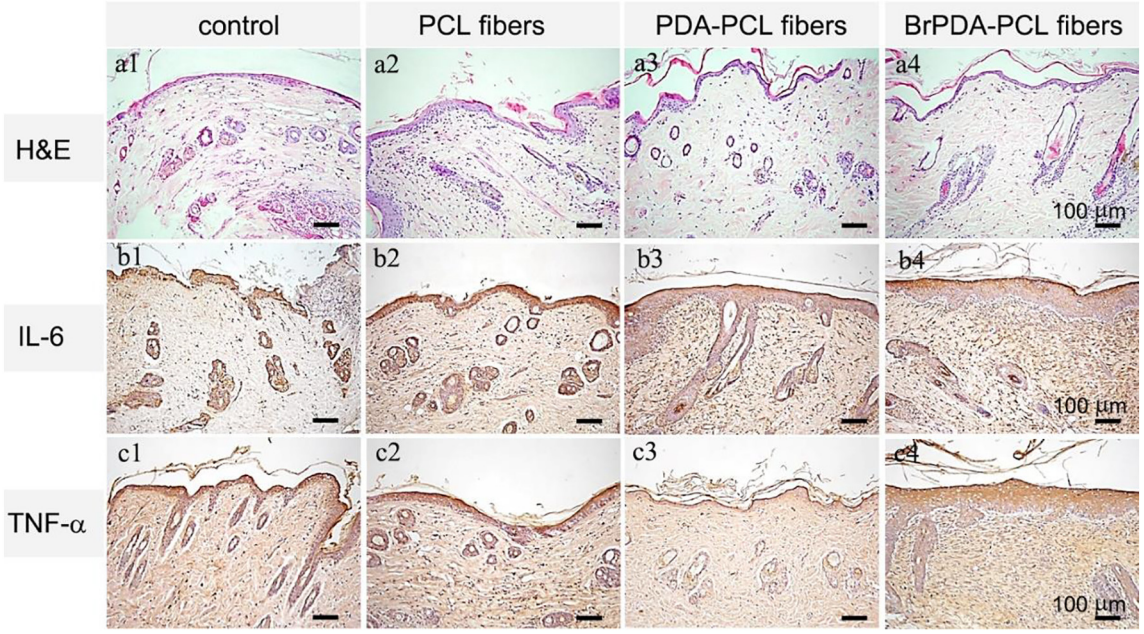

Fig. 10. Histologic H&E staining (a), and IHC staining for IL-6 (b) and TNF-α (c) in healed wound sections.

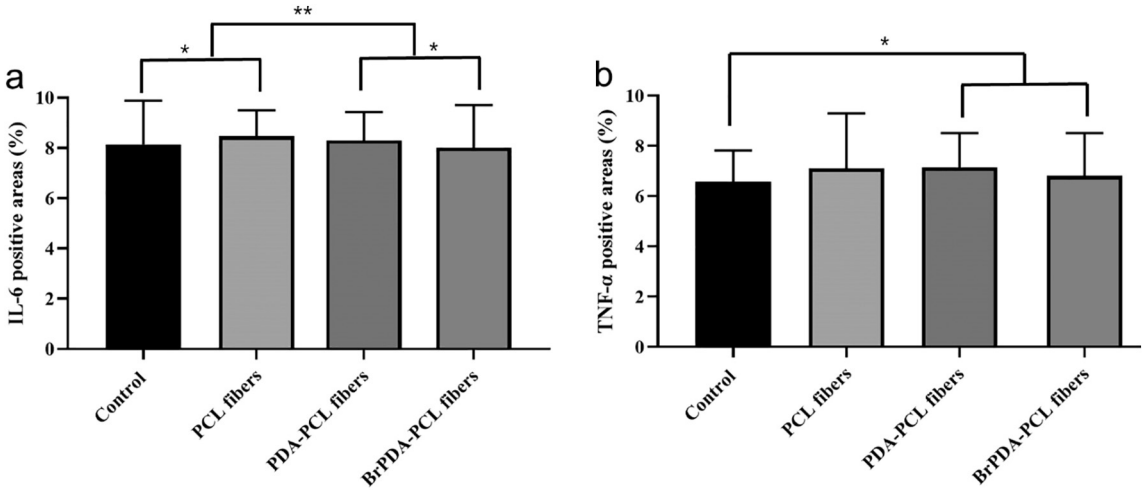

Fig. 11. Quantitative statistical analysis of IL-6 (a) and TNF-α (b) relative area percentage. *p < 0.05, **p < 0.01.

showed the lowest expression of IL-6 and TNF-α (Fig. 11), which was probably due to the introduction of bromelain and PDA that can endow the antibacterial ability to BrPDA-PCL fibers to reduce inflammation. This thus suggests that BrPDA-PCL fibers do not readily induce infection. Both IL-6 and TNF-α can promote somatostatin release, thereby inhibiting growth factor release and wound healing. As BrPDA-PCL fibers did not induce these inflammatory cytokines, these fibers may be suitable as wound dressings.

4. Conclusions

Herein we found that using PDA to immobilize bromelain onto electrospun PCL fibers resulted in the production of membranes that were highly effective wound dressings. Bromelain activity was markedly stabilized via the immobilization process, and the resultant BrPDA-PCL fibers were capable of supporting both cellular adhesion and proliferation. Given the observed synergy between PDA and bromelain, these BrPDA-PCL fibers also exhibited antibacterial activity. When utilized in a rat model of wound healing, inflammation was reduced and healing rates were improved in rats treated using BrPDA-PCL fibers relative to untreated controls. We therefore propose that future studies further examine the value of bromelain-immobilized electrospun PCL fibers as a means of enhancing epithelial regeneration.

CRediT authorship contribution statement

Xinxin Chen: Investigation, Data curation, Writing - original draft. **Xiang Wang:** Data curation. **Siyu Wang:** Investigation. **Xiuhang Zhang:** Investigation. **Jiaao Yu:** Project administration, Writing - review & editing. **Ce Wang:** Writing - review & editing, Supervision.

Declaration of competing interest

The authors declare that they have no known competing financial interests or personal relationships that could have appeared to influence the work reported in this paper.

Acknowledgements

This work is supported by the research grants from the National Natural Science Foundation of China (No. 21474043) and Jilin Provincial Industrial Innovation Program (No. 2016C024).

Appendix A. Supplementary data

Supplementary data to this article can be found online at https://doi.org/10.1016/j.msec.2019.110624.

References

[1] S. Gilotra, D. Chouhan, N. Bhardwaj, S.K. Nandi, B.B. Mandal, Potential of silk sericin based nanofibrous mats for wound dressing applications, Mater. Sci. Eng. C Mater. Biol. Appl. 90 (2018) 420–432.
[2] J. Xiao, Y. Zhu, S. Huddleston, P. Li, B. Xiao, O.K. Farha, G.A. Ameer, Copper metal – organic framework nanoparticles stabilized with folic acid improve wound healing in diabetes, ACS Nano 12 (2018) 1023–1032.
[3] R. Zhao, X. Li, B.L. Sun, Y. Zhang, D. Zhang, Z. Tang, X. Chen, C. Wang, Electrospun chitosan/sericin composite nanofibers with antibacterial property as potential wound dressings, Int. J. Biol. Macromol. 68 (2014) 92–97.
[4] P. Hubner, N. Donati, L.K.M. QuinesIsabel, C.T. Nilson, R. Marcilio, Gelatin-based films containing clinoptilolite-Ag for application as wound dressing, Mater. Sci. Eng. C Mater. Biol. Appl. 107 (2020) 110215.
[5] J.P. Han, L.K. Xiong, X.Y. Jiang, X.Y. Yuan, Y. Zhao, D.Y. Yang, Bio-functional electrospun nanomaterials: from topology design to biological applications, Prog. Polym. Sci. 91 (2019) 1–28.
[6] S.P. Miguel, D.R. Figueira, D. Simoes, M.P. Ribeiro, P. Coutinho, P. Ferreira, I.J. Correia, Electrospun polymeric nanofibres as wound dressings: a review, Colloids Surf. B Biointerfaces 169 (2018) 60–71.
[7] R. Zhao, X. Li, B. Sun, Y. Tong, Z.Q. Jiang, C. Wang, Nitrofurazone-loaded electrospun PLLA/sericin-based dual-layer fiber mats for wound dressing applications, RSC Adv. 5 (2015) 16940–16949.
[8] S.Y. Abdalkarim, H.Y. Yu, D.C. Wang, J.M. Yao, Electrospun poly(3-hydroxybutyrate-co-3-hydroxy-valerate)/cellulose reinforced nanofibrous membranes with ZnO nanocrystals for antibacterial wound dressings, Cellulose 24 (2017) 2925–2938.
[9] L.L. Lima, T.B. Taketa, M.M. Beppu, I.M.O. Sousa, M.A. Foglio, A.M. Moraes, Coated electrospun bioactive wound dressings: mechanical properties and ability to control lesion microenvironment, Mater. Sci. Eng. C Mater. Biol. Appl. 100 (2019) 493–504.
[10] X. Sun, K. Li, S. Chen, B. Yao, Y. Zhou, S. Cui, J. Hu, Y. Liu, Rationally designed particle preloading method to improve protein delivery performance of electrospun polyester nanofibers, Int. J. Pharm. 512 (2016) 204–212.
[11] J. Wan, J. Guo, Z. Miao, X. Guo, Reverse micellar extraction of bromelain from pineapple peel - effect of surfactant structure, Food Chem. 197 (2016) 450–456.
[12] J.A. Ataide, E.F. Gerios, P.G. Mazzola, E.B. Souto, Bromelain-loaded nanoparticles: a comprehensive review of the state of the art, Adv. Colloid Interf. Sci. 254 (2018) 48–55.
[13] Y. Shoham, Y. Krieger, E. Tamir, E. Silberstein, A. Bogdanov-Berezovsky, J. Haik, L. Rosenberg, Bromelain-based enzymatic debridement of chronic wounds: a preliminary report, Int. Wound J. 15 (2018) 769–775.
[14] S. Bayat, N. Amiri, E. Pishavar, F. Kalalinia, J. Movaffagh, M. Hahsemi, Bromelain-loaded chitosan nanofibers prepared by electrospinning method for burn wound healing in animal models, Life Sci. 229 (2019) 57–66.
[15] E. Shoba, R. Lakra, K.M. Syamala, P.S. Korrapati, Fabrication of core-shell nanofibers for controlled delivery of bromelain and salvianolic acid B for skin regeneration in wound therapeutics, Biomed. Mater. 12 (2017) 035005.
[16] C. Qi, L.H. Fu, H. Xu, T.F. Wang, J. Lin, P. Huang, Melanin/polydopamine-based nanomaterials for biomedical applications, Sci. China Chem. 62 (2019) 162–188.
[17] I.S. Kwon, C.J. Bettinger, Polydopamine nanostructures as biomaterials for medical applications, J. Mater. Chem. B 6 (2018) 6895–6903.

[18] Y. Zhang, L. Lu, Y. Chen, J. Wang, Y. Chen, C. Mao, M. Yang, Polydopamine modification of silk fibroin membranes significantly promotes their wound healing effect, Biomater. Sci. 7 (2019) 5232–5237.
[19] C.Y. Liu, C.J. Huang, Functionalization of polydopamine via the Aza-Michael reaction for antimicrobial interfaces, Langmuir 32 (2016) 5019–5028.
[20] Y.H. Ding, M. Floren, W. Tan, Mussel-inspired polydopamine for bio-surface functionalization, Biosurf. Biotribol. 2 (2016) 121–136.
[21] T.T. Zhang, Y.P. Li, W.Y. Hong, Z.Y. Chen, P.Y. Peng, S.L. Yuan, J.Y. Qu, M. Xiao, L. Xu, Glucose oxidase and polydopamine functionalized iron oxide nanoparticles: combination of the photothermal effect and reactive oxygen species generation for dual-modality selective cancer therapy, J. Mater. Chem. B 7 (2019) 2190–2200.
[22] D. Li, Z. Fang, H. Duan, L. Liang, Polydopamine-mediated synthesis of core-shell gold@calcium phosphate nanoparticles for enzyme immobilization, Biomater. Sci. 7 (2019) 2841–2849.
[23] Y.M. Li, X. Li, R. Zhao, C. Wang, F.P. Qiu, B.L. Sun, H. Ji, J. Qiu, Enhanced adhesion and proliferation of human umbilical vein endothelial cells on conductive PANI-PCL fiber scaffold by electrical stimulation, Mater. Sci. Eng. C Mater. Biol. Appl. 72 (2017) 106–112.
[24] M. Haffner-Luntzer, A. Heilmann, A.E. Rapp, R. Roessler, T. Schinke, M. Amling, A. Ignatius, A. Liedert, Antagonizing midkine accelerates fracture healing in mice by enhanced bone formation in the fracture callus, Br. J. Pharmacol. 173 (2016) 2237–2249.
[25] S.M. Eskitoros-Togay, Y.E. Bulbul, S. Tort, F. Demirtas Korkmaz, F. Acarturk, N. Dilsiz, Fabrication of doxycycline-loaded electrospun PCL/PEO membranes for a potential drug delivery system, Int. J. Pharm. 565 (2019) 83–94.
[26] Y.Z. Li, R. Zhao, S. Chao, B.L. Sun, C. Wang, X. Li, Polydopamine coating assisted synthesis of MnO2 loaded inorganic/organic composite electrospun fiber adsorbent for efficient removal of Pb^{2+} from water, Chem. Eng. J. 344 (2018) 277–289.
[27] X. Xu, R. Liu, P. Guo, Z. Luo, X. Cai, H. Shu, Y. Ge, C. Chang, Q. Fu, Fabrication of a novel magnetic mesoporous molecularly imprinted polymer based on pericarpium granati-derived carrier for selective absorption of bromelain, Food Chem. 256 (2019) 91–97.
[28] J.R. Dias, S. Baptista-Silva, C.M.T. de Oliveira, A. Sousa, A.L. Oliveira, P.J. Bartolo, P.L. Granja, In situ crosslinked electrospun gelatin nanofibers for skin regeneration, Eur. Polym. J. 95 (2017) 161–173.
[29] N. Chinatangkul, S. Tubtimsri, D. Panchapornpon, P. Akkaramongkolporn, C. Limmatvapirat, S. Limmatvapirat, Design and characterisation of electrospun shellac-polyvinylpyrrolidone blended micro/nanofibres loaded with monolaurin for application in wound healing, Int. J. Pharm. 562 (2019) 258–270.
[30] S. Chao, Y.M. Li, R. Zhao, L. Zhang, Y.Z. Li, C. Wang, X. Li, Synthesis and characterization of tigecycline-loaded sericin/poly(vinyl alcohol) composite fibers via electrospinning as antibacterial wound dressings, J. Drug Delivery Sci. Technol. 44 (2018) 440–447.
[31] J. Aragón, C. Costa, I. Coelhoso, G. Mendoza, A. Aguiar-Ricardo, S. Irusta, Electrospun asymmetric membranes for wound dressing applications, Mater. Sci. Eng. C Mater. Biol. Appl. 103 (2019) 109822.
[32] Z. Xia, G. Liu, Y. Dong, Y. Zhang, Anticorrosive epoxy coatings based on polydopamine modified molybdenum disulfide, Prog. Org. Coat. 133 (2019) 154–160.
[33] S. Zahid, H. Khalid, F. Ikram, H. Iqbal, M. Samie, L. Shahzadi, A.T. Shah, M. Yar, A.A. Chaudhry, S.J. Awan, A.F. Khan, I.U. Rehman, Bi-layered alpha-tocopherol acetate loaded membranes for potential wound healing and skin regeneration, Mater. Sci. Eng. C Mater. Biol. Appl. 101 (2019) 438–447.
[34] D. Simões, S.P. Miguel, M.P. Ribeiro, P. Coutinho, A.G. Mendonça, I.J. Correia, Recent advances on antimicrobial wound dressing: a review, Eur. J. Pharm. Biopharm. 127 (2018) 130–141.
[35] H. Liu, X. Qu, H. Tan, J. Song, M. Lei, E. Kim, G.F. Payne, C. Liu, Role of polydopamine's redox-activity on its pro-oxidant, radical-scavenging, and antimicrobial activities, Acta Biomater. 88 (2019) 181–196.
[36] J.A. Ataide, N.N. de Carvalho, M.A. Rebelo, M.V. Chaud, D. Grotto, M. Gerenutti, M. Rai, P.G. Mazzola, A.F. Jozala, Bacterial nanocellulose loaded with bromelain: assessment of antimicrobial, antioxidant and physical-chemical properties, Sci. Rep. 7 (2017) 18031.